

# Detection of Word Adversarial Examples in NLP: Benchmark and Baseline via Robust Density Estimation

Anonymous ACL submission

## Abstract

Word-level adversarial attacks have shown success in NLP models, drastically decreasing the performance of transformer-based models in recent years. As a countermeasure, adversarial defense has been explored, but relatively few efforts have been made to detect adversarial examples. However, detecting adversarial examples in NLP may be crucial for automated task (e.g. review sentiment analysis) that wishes to amass information about a certain population and additionally be a step towards a robust defense system. To this end, we release a dataset for four popular attack methods on four datasets and four NLP models to encourage further research in this field. Along with it, we propose a competitive baseline based on density estimation that has the highest AUC on 29 out of 30 dataset-attack-model combinations.<sup>1</sup>

## 1 Introduction

Adversarial examples in NLP refer to seemingly innocent texts that alter the model prediction to a desired output, yet remain imperceptible to humans. In recent years, word-level adversarial attacks have shown success in NLP models, drastically decreasing the performance of transformer-based models in sentence classification tasks with increasingly smaller perturbation rate (Jin et al., 2020; Li et al., 2020; Garg and Ramakrishnan, 2020; Ren et al., 2019). In the image domain, two main lines of research exist to counteract adversarial attacks : adversarial example *detection* and *defense*. The goal of detection is to discriminate an adversarial input from a normal input, whereas adversarial defense intends to predict the correct output of the adversarial input. While works defending these attacks have shown some progress in NLP (Zhou et al., 2021; Keller et al., 2021; Jones et al., 2020), only few efforts have been made in techniques for the sole purpose of detection.

<sup>1</sup><https://github.com/anonymous92874838/text-adv-detection>

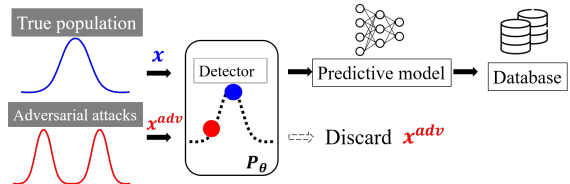


Figure 1: Schematic Diagram of our adversarial detection Framework. We propose a density estimation model to detect adversarial samples.

However, detecting adversarial examples in NLP may be as crucial as defending them in certain applications, in which alerting the victim the existence of adversarial samples suffices. For instance, models used for automation of tasks (e.g. review sentiment analysis, news headline classification, etc) are adopted to efficiently gain information about the true data-generating population (e.g. consumers, news media, etc), rather than the adversary. For such applications, attaining outputs of an adversarial input - whether correct or not - may turn out to be harmful to the system. Accordingly, the *discard-rather-than-correct strategy* which simply discards the detected adversarial input would be a good countermeasure. Moreover, being able to detect adversarial examples may be a step towards building a more robust defense model as the popular defense paradigm, adversarial training, usually suffers from degraded performance on normal inputs (Bao et al., 2021). With a competent detection system, the normal and adversarial inputs can be processed by two separate mechanisms as proposed by Zhou et al. (2019).

Many existing works in NLP that employ detection as an auxiliary task for defense require adversarial samples for training, which may be restrictive scenario given the variety of attack methods and sparsity of adversarial samples in the real world. In addition, some works either focus on a single type of attack or is limited to character-level attacks, both of which do not abide the two key constraints (semantics and grammaticality) in order to

Method	Summary	Require Train Data?	Require Val. Data?	Target Attacks <sup>†</sup>
RDE (Ours)	Feature-based density estimation			Token-level
Mozes et al. (2021, FGWS)	Word frequency-based		✓	Word-level
Bao et al. (2021, ADFAR)	Learning-based (sentence-level)	✓	✓	Word-level
Le et al. (2021, DARCY)	Learning-based (Honeypot)	✓	✓	Wallace et al. (2019)
Zhou et al. (2019, DISP)	Learning-based (token-level)	✓	✓	Token-level
Pruthi et al. (2019)	Learning-based (Semi-character RNN)	✓	✓	Char-level

Table 1: Key characteristics of the detection methods in the NLP domain. Requiring training/validation data means adversarial samples are needed for training/validation. Token-level encompasses word and character-level. <sup>†</sup>Determined by the experimented types of attacks. Some works can be trivially modified to adjust to a different type of attacks.

072 be imperceptible (Morris et al., 2020a). As opposed  
073 to this, carefully crafted word-level adversarial at-  
074 tacks can maintain original semantics and remain  
075 unsuspecting to human inspectors. To encourage  
076 further research in this domain, we release a bench-  
077 mark for word-level adversarial example detection  
078 on four attack methods across four NLP models  
079 and four datasets. We also propose a simple but  
080 effective detection method that utilizes density es-  
081 timation in the feature space as shown in Fig. 1  
082 without any assumption of the attack algorithm or  
083 requiring adversarial samples for training or vali-  
084 dation. We summarize the existing works in Table  
085 1.

086 As opposed to a recent work (Mozes et al., 2021),  
087 which rely on word frequency to assess the like-  
088 lihood of sentence(s), we model the probability  
089 density of the entire sentence(s). To achieve this,  
090 we fit a parametric density estimation model to  
091 the features obtained from a classification model  
092 (e.g. BERT) to yield likelihoods of each sample  
093 as shown by Fig. 2 inspired by classic works in  
094 novelty detection (Bishop, 1994), which utilizes  
095 generative models to find anomalies. However, sim-  
096 ply fitting a parametric model suffers from curse  
097 of dimensionality characterized by (i) sparse data  
098 points and spurious features (ii) and rare outliers  
099 that hamper accurate estimation. To tackle these is-  
100 sues, we leverage classical techniques in statistical  
101 analysis, namely kernel PCA and Minimum Co-  
102 variance Determinant, for robust density estimation  
103 (RDE).

104 Our attack-agnostic and model-agnostic detec-  
105 tion method achieves best performance as of AUC  
106 on 29 out of 30 dataset-attack-model combinations  
107 and best performance as of TPR, F1, AUC on 25 of  
108 them without any assumption on the attacks.

109 Our contributions are two-fold:

- 110 • We propose a adversarial detection method that  
111 does not require validation sets of each attack

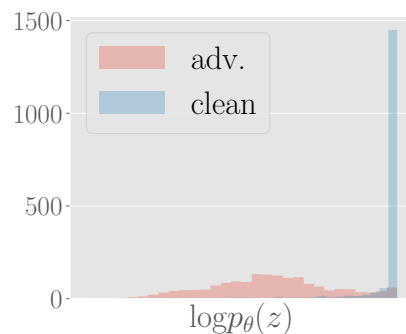


Figure 2: Density estimation using our method in (Data-Attack-Model) = (IMDB-(TF-adj)-BERT). Normal samples are peaked at high likelihood region. Adversarial samples tend to have low likelihood.

112 method through robust parameter estimation by  
113 alleviating problems caused by curse of dimen-  
114 sionality.

- 115 • We release a dataset for word-level adversarial  
116 example detection on 4 attacks, 4 datasets, and  
117 4 models and the source code for experimenting  
118 on various experimental protocols.

119 We further provide analysis on a stronger adversary  
120 with partial knowledge of the detection method and  
121 techniques to counteract the adversary. Last, we  
122 investigate the proposed method’s applicability on  
123 character-level attacks.

## 124 2 Preliminaries

### 125 2.1 Adversarial Examples

126 Given an input space  $\mathcal{X}$ , a label space  $\mathcal{Y}$ , a predic-  
127 tive model  $\mathcal{F} : \mathcal{X} \rightarrow \mathcal{Y}$ , and an oracle model  
128  $\mathcal{F}^* : \mathcal{X} \rightarrow \mathcal{Y}$ , a successful adversarial example  
129  $x_{\text{adv}}$  of an input  $x \in \mathcal{X}$  satisfies the following:

$$130 \mathcal{F}^*(x) = \mathcal{F}(x) \neq \mathcal{F}(x_{\text{adv}}),$$

$$131 C_i(x, x_{\text{adv}}) = 1 \text{ for } i \in \{1, \dots, c\} \quad (1)$$

Dataset	Topic	Task	Classes	Median Length	# of Test Samples Original / Generated
IMDB(Maas et al., 2011)	movie review	sentiment classification	2	161	25K / 10K
AG-News(Zhang et al., 2015)	news headline	topic classification	4	44	7.6K / 7.6K
SST-2(Socher et al., 2013)	movie review	sentiment classification	2	16	2.7K / 2.7K
YELP(Zhang et al., 2015)	restaurant review	sentiment classification	2	152	38K / 5K

Table 2: Summary of the benchmark dataset. For SST-2, 0.87K held-out validation samples and 1.8K test samples are used.

where  $C_i$  is an indicator function for the  $i$ -th constraint between the perturbed text and the original text, which is 1 when the two texts are indistinguishable with respect to the constraint. The constraints vary from attack algorithms and is crucial for maintaining the original semantics while providing an adequate search space. For instance, Jin et al. (2020) ensure that the embedding of the two sentences have a cosine similarity larger than 0.5 using the Universal Sentence Encoder (Cer et al., 2018, USE).

## 2.2 Detecting Adversarial Examples

For the purpose of detecting adversarial examples, a dataset  $\mathcal{D}$  consisting of clean samples ( $\mathcal{D}_{\text{clean}}$ ) and adversarial samples ( $\mathcal{D}_{\text{adv}}$ ) is required. The details of the configuration induce a scenario such as whether the original text of adversarial samples overlap with the clean samples, the ratio of clean and adversarial samples, etc. However, this has rarely been discussed in detail and the exact implementation varies by works. In all the main experiments, we follow the configuration (described below) used in a seminal work Xu et al. (2018) on adversarial example detection in the image domain. We denote the test set as  $\mathcal{X}_t$  and the correctly classified test set as  $\mathcal{X}_c \subset \mathcal{X}_t$ .

- Configuration 1 : Sample disjoint subsets  $\mathcal{S}_1, \mathcal{S}_2 \subset \mathcal{X}_t$ . For the correctly classified examples of  $\mathcal{S}_1$ , adversarial attacks are generated and the successful examples form  $\mathcal{D}_{\text{adv}}$ .  $\mathcal{D}_{\text{clean}}$  is formed from  $\mathcal{S}_2$ .

More discussion regarding the other configuration and experiment results is in Appendix A.2.

## 3 Method

### 3.1 Benchmark

We generate adversarial examples on 4 models, 4 types of attacks, and 4 sentence classification datasets. Since some attacks (Garg and Ramakrishnan, 2020) require hundreds of queries and inference of models per query, vast amount of time

is required to create all the adversarial examples (e.g. up to 44 hours for 5,000 examples on the IMDB dataset using TF-adjusted attack). This renders on-the-fly generation and detection of adversarial examples extremely inefficient. Therefore, adversarial examples are created beforehand and sampled according to Section 2.2. Four sentence classification datasets (IMDB, AG-News, SST-2, Yelp) are chosen to have diverse topics and length. See Table 2 for the summary and the number of generated samples.

We choose two non-transformer-based models (Word-CNN Kim (2014); LSTM Hochreiter and Schmidhuber (1997)) and two transformer-based models (RoBERTa Liu et al. (2019); BERT Devlin et al. (2018)). Recently, numerous adversarial attacks have been proposed. We choose two widely known attacks called Textfooler (Jin et al., 2020, TF) and Probability Weighted Word Saliency (Ren et al., 2019, PWWS) and a recent approach using BERT to generate attacks called BAE (Garg and Ramakrishnan, 2020). Lastly, we also include a variant of TF called TF-adjusted (Morris et al., 2020a, TF-adj), which enforces a stronger similarity constraint to ensure imperceptibility to humans. All attacks are created using the TextAttack library (Morris et al., 2020b). See Appendix A.1 for the summary of attack methods and Appendix A.6 for a code snippet of using our benchmark.

### 3.2 Estimating Density and Parameters in Feature Space

Earlier works in novelty detection (Bishop, 1994) have shown that generative models fitted on normal samples are capable of detecting unseen novel samples (e.g. adversarial samples). Since we can assume that the training samples, which were used to train the victim model of a particular task, are available to the victim party, we can similarly design a generative model that estimates input density. However, directly using the inputs is challenging as modeling the probability distribution of raw texts is non-trivial. To bypass this, we fit a paramet-

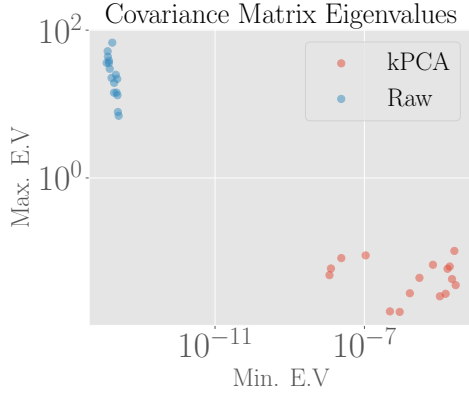


Figure 3: Comparisons of the maximum and minimum eigenvalues of the estimated covariance matrices for RoBERTa and BERT across all datasets and classes (20 samples total). Naive estimation (blue) using raw features leads to extremely ill-conditioned matrices while kPCA (red) alleviates this.

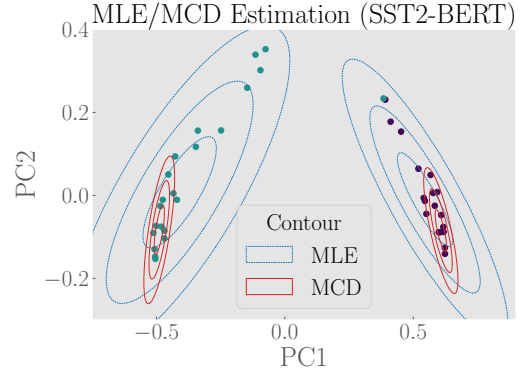


Figure 4: Probability-contours of  $\tilde{\Sigma}$  within three standard deviations estimated by MLE and Minimum Covariance Determinant (MCD) of BERT on SST-2 dimensionality reduced by kPCA. Colors of the points indicate class. See Sec. 3.3 for details.

ric density estimation model in the feature space (i.e. penultimate layer of the classification model). Since a neural network learns to extract important features of the inputs to distinguish classes, the features can be regarded as representations of the raw inputs. For a pre-trained predictive model  $\mathcal{F}$ , let  $z \in \mathcal{Z} \subset \mathbb{R}^D$  denote the feature given by the feature extractor  $\mathcal{H} : \mathcal{X} \rightarrow \mathcal{Z}$ . Then the entire predictive model can be written as the composition of  $\mathcal{H}$  and a linear classifier.

Given a generative model  $p_\theta$  with mean and covariance as parameters  $\theta = (\mu, \Sigma)$ , we can use the features of the training samples ( $\mathcal{X}_{train}$ ) to estimate the parameters. Then, novel adversarial samples lying in the unobserved feature space are likely to be assigned a low probability, because the generative model only used the normal samples for parameter fitting. For simplicity, we assume the distributions of the feature  $z$  follow a multivariate Gaussian, and thus we model the class conditional probability as  $p_\theta(z|y = k) \sim N(\mu_k, \Sigma_k) \propto \exp\{-\frac{1}{2}(z - \mu_k)^T \Sigma_k^{-1} (z - \mu_k)\}$ , where  $y$  indicates the class of a given task. Then, the maximum likelihood estimate (MLE) is given by the sample mean  $\tilde{\mu}_{MLE} = \frac{1}{N} \sum_{i=1}^N z_i$  and sample covariance  $\tilde{\Sigma}_{MLE} = \frac{1}{N-1} \sum_{i=1}^N (z_i - \tilde{\mu}_{MLE})(z_i - \tilde{\mu}_{MLE})^T$ .

However, accurate estimation of the parameters is difficult with finite amount of samples especially in high dimensions ( $D = 768$  for transformer-based models) due to curse of dimensionality, thereby (i) leading to sparse data points and spurious features (ii) and occasional outliers that influence the parameter estimates. In Figure 3, we empirically show that the covariance matrices (blue)

of BERT and RoBERTa across all models across all datasets are ill-conditioned, demonstrated by the high maximum eigenvalues and extremely small minimum eigenvalues ( $\approx 10^{-12}$ ). Due to this, the precision matrix is abnormally inflated in certain dimensions and prone to numerical errors during inversion. More analysis regarding the upperbound of this error is provided in Appendix A.3.

In addition, although we have assumed a Gaussian distribution for convenience, the unknown true distribution may be a more general elliptical distribution with thicker tails. This is observed empirically in Figure 4 by visualizing the features into two dimensions by dimensionality reduction. Outliers that are far from the modes of both classes (indicated by color) are present: those that are completely misplaced occasionally exist, while subtle outliers that deviate from the Gaussian distribution assumption are common, which influences the MLE estimation. Thus, to accurately estimate the Gaussian parameters, these outliers should be taken into account. In the following subsection, we tackle these issues through well-known classical techniques from statistical analysis.

### 3.3 RDE using kPCA and Minimum Covariance Determinant

To address the first issue, we first use kernel PCA (Schölkopf et al., 1998, kPCA) to select top  $P$  orthogonal bases that best explain the variance of the data, thereby reducing redundant features. Given  $N$  centered samples  $Z_{train} \in \mathbb{R}^{D \times N} = [z_1, \dots, z_N]$ , a mapping function  $\phi : \mathbb{R}^D \rightarrow \mathbb{R}^{D'}$ , and its mapping applied to each sample  $\Phi(Z_{train}) \in \mathbb{R}^{D' \times N}$ , kPCA projects the data points to the eigenvec-



tors with the  $P$  largest eigenvalues of the covariance  $\Phi(Z_{\text{train}})\Phi(Z_{\text{train}})^T$ <sup>2</sup>. Intuitively, this retains the most meaningful feature dimensions, which explains the data the most, while reducing spurious features and improve stability of inversion by decreasing the condition number as shown in Figure 3. By leveraging non-linear  $\phi$ , we are able to find meaningful non-linear signals in the features as opposed to standard PCA. We use the radial basis function as our kernel. Comparison of performance with standard PCA is provided in Appendix Table A.5. For a complete derivation, please refer to Schölkopf et al. (1997).

However, this does not remove sample-level outliers as shown in Figure 4. Since we have assumed a Gaussian distribution, "peeling off" outliers may be favorable for parameter estimation. A principled way of removing outliers for parameter estimation has been an important research area in multivariate statistics and various methods have been developed for robust covariance estimation (Friedman et al., 2008; Ledoit and Wolf, 2004). Among them, Minimum Covariance Determinant (Rousseeuw, 1984, MCD) finds a subset of  $h \leq N$  samples that minimizes the determinant of  $\Sigma$ .<sup>3</sup> As the determinant is proportional to the differential entropy of a Gaussian up to a logarithm (shown in Appendix A.4), this results in a robust covariance estimation consisting of centered data points rather than outliers. For a review, see Hubert et al. (2018). Qualitatively, we observe in Figure 4 that MLE estimates have their means yanked towards the outliers and that the contours are disoriented (Blue). MCD estimates (Red) focus on the high density clusters, which leads to higher performance as will be shown in the experiments.

In summary, we retain informative features by applying kPCA and obtain robust covariance estimates by using MCD on the train set. Using the estimated robust parameters, we can evaluate the likelihood of a test sample. We treat those with low likelihood as novel (adversarial) samples. Our algorithm is shown in Algorithm 1 in the Appendix. We empirically validate the effectiveness of two techniques and discuss the effect of hyper-parameter  $P$  and  $h$  in the following sections.

<sup>2</sup>For simplicity, we assume  $\Phi(Z_{\text{train}})$  is centered. When this assumption does not hold, slightly modified approach is taken. See Appendix B of Schölkopf et al. (1998) for details.

<sup>3</sup>Although the possible number of subsets is infeasibly large, Rousseeuw and Driessen (1999) propose an iterative method that converges relatively fast for  $\approx 4000$  samples with 100 dimensions.

## 4 Experiments 327

### 4.1 Experimental Settings 328

We experiment on the four datasets (IMDB, AG-News, SST-2, Yelp) and four attack methods described in Section 3.1. Our experiment is based on BERT and RoBERTa as they are widely used competent models for various tasks. Since SST-2 only has 1.8K test samples, TF-adjusted attack was unable to create an adequate number of successful adversarial samples (e.g. 80 samples out of 1.7K). Omitting experiments for these, there are 22 combinations of dataset-attack-model in total. 329  
330  
331  
332  
333  
334  
335  
336  
337  
338

In addition, we (i) investigate a potential adversary with partial/full knowledge of the detection method and (ii) conduct experiments on a character level attack (Appendix A.10) to demonstrate the applicability of our method. Last, we discuss more realistic scenarios for further study and conduct hyper-parameter and qualitative analysis. 339  
340  
341  
342  
343  
344  
345

### 4.2 Compared Methods 346

We compare our robust density estimation method (RDE) with a recently proposed detection method in NLP called FGWS (Mozes et al., 2021) which is a word frequency-based method that assumes that rare words appear more often in adversarial samples. We also verify whether Perplexity (PPL) computed by a language model (GPT-2, Radford et al. 2019) is able to distinguish normal and adversarial samples as PPL is often used to compare the fluency of the two samples. FGWS implicitly models the input density via word frequencies, while GPT-2 explicitly computes the conditional probability via an auto-regressive tasks. In addition, we adopt Lee et al. (2018) denoted as MLE, which is a out-of-distribution detector from the image domain. Similar to RDE, Lee et al. (2018) fits a Gaussian model using the maximum likelihood estimation (MLE) then trains a logistic regressor using the likelihood scores. Since we assume that adversarial samples are not available for training, we do not train a regression model, but only use the likelihood score. For further details, see Section 5. We compare MLE with two variants of our method: 347  
348  
349  
350  
351  
352  
353  
354  
355  
356  
357  
358  
359  
360  
361  
362  
363  
364  
365  
366  
367  
368  
369

- **RDE(-MCD)** : This is a variant of RDE, in which only kPCA is applied to the features without MCD. The results of applying standard PCA instead of kPCA are reported in Table A.5 of Appendix. 370  
371  
372  
373  
374
- **RDE** : After applying kPCA, MCD estimate is 375

used. This is the final proposed robust density estimation incorporating both kPCA and MCD.

### 4.3 Evaluation Metric and Protocol

Following Xu et al. (2018), we report three widely used metrics in adversarial example detection : (1) *True positive rate* (TPR) is the fraction of true adversarial samples out of predicted adversarial samples. (2) *F1-score* (f1) measures the harmonic mean of precision and recall. Since all compared methods are threshold-based methods, we report TPR at a fixed false positive rate (FPR). (3) *Area under ROC* (AUC) measures the area under TPR vs. FPR curve. For all three metrics, higher denotes better performance.

Note that whereas AUC considers performance on various FPR's, TPR and F1 is dependent on one particular FPR. In all our experiments, we fixed FPR= 0.1, which means 10% of normal samples are predicted to be adversarial samples. This threshold should be chosen depending on the context (i.e. the degree of safety-criticalness). We believe this standard should be elevated as more works are proposed in the future. For IMDB and AG-News, 30% of the test set is held out as validation set for Mozes et al. (2021). We subsample out of the test set as described in Section 2.2. For quantitative analysis, we report the mean and its standard error of three repetitions of random seeds for test/validation split and subsampled samples.

### 4.4 Implementation Details

We choose the feature  $z$  to be the output of the last attention layer (before Dropout and fully connected layer) for BERT and RoBERTa. RDE has two main hyper-parameters, namely the number of retained dimensions  $P$  of kPCA and the support fraction  $h$  of MCD. We fix  $P = 100$  for all experiments as we observe the performance is not sensitive to  $P$ . For  $h$ , we use the default value proposed in the algorithm, which is  $\frac{N+P+1}{2N}$ . We study the effect of  $h$  in Section 4.6. All models are pre-trained models provided by TextAttack and both kPCA and MCD are implemented using scikit-learn (Pedregosa et al., 2011). We use the radial basis function as our kernel. The time required to estimate the parameters of our method is approximately around 25 seconds. For more details, see Appendix A.5.

For FGWS, we use the official implementation<sup>4</sup> and use the held-out validation set of each attack

<sup>4</sup><https://github.com/maximilianmozes/fgws>

to tune the threshold for word frequency  $\delta$  as done in the original work. For PPL, we use the Hugging-Face (Wolf et al., 2020) implementation of GPT-2 (Radford et al., 2019).

### 4.5 Results

#### Static Adversary

Table 3 demonstrates the results on three datasets and four attacks. Results on Yelp are presented in Appendix Tab. A.6 . The highest means out of the four methods are written in bold. Out of the 30 combinations of dataset-attack-model, RDE achieves the best performance on 29 of them on AUC and 25 of them for all three metrics, which shows the competitiveness of our simple method. The motivation of our method is verified by the large margin of improvement from MLE in almost all cases. Using MCD estimation also further improves performance except in the few cases of AG-News. FGWS generally has a higher performance compared to PPL, but is inferior to MLE in most cases. Note the degradation of performance in FGWS for BAE and TF-adj, which are more subtle attacks with stronger constraint, as FGWS relies on use of rare words. This trend is not observed in feature density-based methods (MLE and RDE).

FGWS outperforms ours on TPR and F1 in five combinations out of 30, but our method has higher AUC on four of them. Interestingly, all the five results are from PWWS attacks, which indicates that our method is relatively susceptible to PWWS. Nonetheless, AUC still remains fairly high: On IMDB and AG-News, the AUC's are all over 0.9. On the other hand, all methods have degraded performance on SST-2, which may be due to shorter sentence lengths. Some examples of ROC curves are presented in Appendix A.8. Improving detection rate in SST-2 is left as a future work.

**Adaptive Adversary** In this section, we assume that the adversary is aware of the detection method, but does not have full access to the model parameters. Being conscious of the fact that RDE relies on the discriminative feature space, the adversary does not terminate once the attacked sample reaches the decision boundary, but goes on to generate samples that are closer to the feature space of the incorrect target until a given threshold. Such attacks that increase the number of trials have been similarly applied in Xie et al. (2019) to create stronger attacks. As shown in Tab. 4, feature-based methods including RDE shows considerable degradation in

Models	Methods	Attacks											
		TF			PWWS			BAE			TF-adj		
		TPR	FI	AUC	TPR	FI	AUC	TPR	FI	AUC	TPR	FI	AUC
<b>IMDB</b>													
BERT	PPL	48.7±0.2	61.4±0.2	76.9±0.2	37.8±0.5	51.2±0.5	71.7±0.2	27.0±0.5	39.4±0.5	67.3±0.1	24.5±0.8	36.5±1.0	67.9±0.3
	FGWS	84.6±0.3	87.1±0.2	87.1±0.3	<b>88.2±0.1</b>	<b>89.0±0.0</b>	90.8±0.0	62.1±0.3	72.3±0.2	70.9±0.3	72.6±0.9	80.6±0.9	78.4±0.6
	MLE	86.3±1.1	87.9±0.7	94.5±0.2	75.7±1.4	81.5±0.9	92.4±0.2	81.8±1.3	85.3±0.8	93.7±0.2	88.3±1.0	89.1±0.6	95.3±0.2
	RDE(-MCD)	96.3±0.3	93.4±0.2	96.8±0.1	86.9±0.9	88.3±0.5	94.6±0.2	92.5±0.5	91.4±0.3	95.8±0.2	98.2±0.2	94.6±0.2	97.6±0.2
	RDE	<b>96.6±0.2</b>	<b>93.5±0.1</b>	<b>97.7±0.2</b>	87.8±0.4	88.8±0.2	<b>95.2±0.2</b>	<b>93.8±0.1</b>	<b>92.1±0.0</b>	<b>96.9±0.2</b>	<b>98.8±0.0</b>	<b>95.0±0.1</b>	<b>98.7±0.2</b>
RoBERTa	PPL	47.8±0.1	60.6±0.1	78.4±0.1	43.5±0.7	56.7±0.6	76.1±0.2	25.9±0.4	38.2±0.5	67.0±0.2	26.6±0.9	39.0±1.1	69.1±0.4
	FGWS	85.1±0.1	87.4±0.1	88.0±0.1	92.1±0.2	91.4±0.2	93.6±0.2	61.5±0.2	71.8±0.1	70.3±0.1	69.2±0.4	78.0±0.1	75.4±0.2
	MLE	80.5±1.0	84.5±0.6	94.0±0.2	76.8±1.3	82.2±0.8	93.3±0.2	75.5±1.5	81.4±0.9	93.1±0.3	86.4±2.3	88.0±1.3	95.3±0.7
	RDE(-MCD)	98.5±0.1	94.5±0.1	97.9±0.1	95.0±0.3	92.7±0.2	96.7±0.1	<b>95.4±0.4</b>	<b>93.0±0.2</b>	97.0±0.2	98.6±0.4	94.8±0.2	98.1±0.4
	RDE	<b>98.9±0.1</b>	<b>94.7±0.0</b>	<b>98.6±0.1</b>	<b>95.2±0.1</b>	<b>92.8±0.1</b>	<b>97.2±0.1</b>	95.3±0.2	92.9±0.1	<b>97.6±0.1</b>	<b>98.8±0.4</b>	<b>95.9±0.6</b>	<b>99.0±0.2</b>
<b>AG-News</b>													
BERT	PPL	75.7±0.4	81.6±0.2	91.0±0.2	70.8±0.7	78.3±0.5	89.5±0.2	31.2±1.3	44.2±1.4	73.0±0.8	32.8±1.8	45.9±1.9	73.3±0.8
	FGWS	82.4±0.6	85.7±0.3	84.2±0.7	<b>91.0±0.1</b>	<b>90.6±0.1</b>	90.8±0.3	64.3±0.9	73.8±0.6	71.3±0.4	63.8±1.0	74.3±1.0	71.9±0.7
	MLE	77.8±0.5	82.9±0.3	93.5±0.1	70.4±0.9	78.0±0.6	92.0±0.1	72.7±1.8	79.6±1.2	92.8±0.4	71.0±1.6	78.9±0.9	92.0±0.2
	RDE(-MCD)	<b>96.2±0.1</b>	<b>93.3±0.0</b>	<b>97.1±0.1</b>	89.8±0.8	90.0±0.4	<b>95.6±0.1</b>	93.2±0.9	92.1±0.6	96.2±0.3	96.6±1.0	93.6±0.5	96.0±0.1
	RDE	95.8±0.2	93.2±0.1	96.9±0.1	88.7±1.0	89.3±0.6	95.4±0.1	<b>96.6±0.1</b>	<b>93.7±0.1</b>	<b>96.9±0.1</b>	<b>98.2±0.6</b>	<b>95.4±0.3</b>	<b>97.5±0.3</b>
RoBERTa	PPL	77.1±0.5	82.4±0.3	91.8±0.1	72.2±0.8	79.3±0.5	89.6±0.2	37.1±1.4	50.4±1.5	74.7±0.3	31.8±1.3	45.3±1.3	74.3±1.3
	FGWS	78.8±0.5	83.5±0.3	82.2±0.2	<b>86.6±0.4</b>	<b>88.1±0.2</b>	87.9±0.3	53.3±3.4	65.1±2.7	63.5±2.0	58.9±3.4	69.7±2.6	70.1±0.9
	MLE	82.5±0.3	85.7±0.2	94.1±0.1	78.6±0.5	83.4±0.2	92.9±0.2	68.1±3.1	76.3±2.2	91.5±0.7	65.0±2.3	74.4±1.7	91.2±0.2
	RDE(-MCD)	90.5±0.5	90.3±0.3	<b>96.1±0.1</b>	84.1±1.2	86.6±0.7	<b>94.8±0.2</b>	77.8±4.1	82.6±2.6	93.9±0.5	82.6±2.7	85.9±1.5	94.5±0.4
	RDE	<b>92.9±0.3</b>	<b>91.6±0.2</b>	95.7±0.1	84.5±0.8	86.9±0.5	93.9±0.2	<b>89.3±2.3</b>	<b>89.6±1.3</b>	<b>95.3±0.5</b>	<b>94.4±0.7</b>	<b>92.6±0.4</b>	<b>96.0±0.3</b>
<b>SST-2</b>													
BERT	PPL	31.7±0.6	44.8±0.6	73.1±0.3	29.2±1.3	41.9±1.4	73.4±0.4	22.2±1.6	33.5±2.0	67.0±0.5			
	FGWS	60.8±0.4	72.3±0.3	73.6±0.3	<b>79.9±0.6</b>	<b>84.9±0.4</b>	<b>86.7±0.4</b>	34.7±0.3	48.0±0.3	60.3±0.3			
	MLE	33.3±1.3	46.5±1.4	79.8±0.5	23.2±0.4	34.8±0.6	78.4±0.3	32.6±1.3	45.8±1.5	76.8±0.6			
	RDE(-MCD)	61.3±0.8	71.6±0.6	86.3±0.4	46.6±0.7	59.5±0.6	84.6±0.2	45.4±1.3	58.5±1.1	80.6±0.6			
	RDE	<b>66.1±0.8</b>	<b>75.1±0.5</b>	<b>87.7±0.3</b>	54.3±1.1	66.1±0.9	86.6±0.2	<b>48.0±1.4</b>	<b>60.7±1.2</b>	<b>81.0±0.5</b>			
RoBERTa	PPL	34.7±0.7	48.0±0.7	75.0±0.5	32.5±1.6	45.5±1.7	73.9±0.5	20.0±1.3	30.8±1.6	65.3±0.4			
	FGWS	61.6±0.2	73.0±0.1	73.7±0.1	<b>80.8±0.2</b>	<b>85.6±0.1</b>	86.4±0.2	36.1±1.0	49.4±1.1	60.0±0.6			
	MLE	44.2±0.6	57.3±0.5	84.4±0.3	33.1±0.8	46.3±0.8	81.9±0.4	37.1±0.5	50.5±0.5	77.9±0.4			
	RDE(-MCD)	63.2±0.2	73.0±0.1	87.8±0.1	53.1±0.7	65.1±0.6	85.4±0.2	45.7±0.7	58.7±0.7	79.3±0.3			
	RDE	<b>74.1±0.3</b>	<b>80.6±0.2</b>	<b>90.4±0.1</b>	67.7±1.1	76.2±0.8	<b>89.1±0.0</b>	<b>52.0±0.3</b>	<b>64.3±0.3</b>	<b>80.6±0.1</b>			

Table 3: Adversarial detection results for BERT and RoBERTa on three datasets on Scenario 1. For all metrics, higher means better.

performance against these attacks, while PPL and FGWS have increased performance. All standard errors are less than 0.3.

Reference	TF-Strong		PWWS-Strong	
	BERT	RoBERTa	BERT	RoBERTa
	97.7	98.6	95.2	97.2
PPL	79.0(+2.1)	84.4(+6.0)	73.7 (+2.0)	81.7 (+5.6)
FGWS	87.9(+0.8)	90.5(+2.5)	92.2(+1.4)	<b>95.3(+1.7)</b>
MLE	93.0(-1.5)	90.4(-3.6)	90.7(-1.7)	90.1(-3.2)
RDE	<u>94.7(-3.0)</u>	<u>92.9(-5.0)</u>	<u>92.4(-2.8)</u>	92.0(-5.2)
RDE+	<b>95.6</b>	<b>94.5</b>	<b>94.2</b>	94.5

Table 4: AUC( $\Delta$ ) for character level attack on IMDB on two adaptive attacks. Reference refers the original RDE against static attacks and  $\Delta$  refers to the absolute decrease in performance compared to its respective reference. RDE+ refers to applying RDE after finetuning the features.

However, to combat these type of attacks, the defender can use few examples of the previously detected static adversarial samples to adjust the feature space. Specifically, the features of the predictive model  $\mathcal{F}_\psi$  (e.g. BERT) is finetuned such that the adversarial samples are located near the decision boundary and far from the classes. To achieve this, the parameters  $\psi$  of the predictive model is trained such that the entropy of the softmax proba-

bility can be maximized.

$$\psi_T = \sum_{t=1}^T [\psi_t + \sum_{x_i \sim \mathcal{D}_{adv}}^b \nabla \mathcal{H}(\mathcal{F}(x_i; \psi_{t-1}))] \quad (2)$$

With only **T=5** iterations and **80** adversarial samples ( $b=16$ ), RDE+ is able to recover some of its performance by adjusting the feature space. Since only few updates are made to the model, the original task performance is negligibly affected (For RoBERTa, 95.1% is marginally increased to 95.2%).<sup>5</sup> Note that only the previously detected static adversarial samples are used to finetune the feature space not the stronger attacks from the adaptive adversary. In addition, stronger attacks are usually more perceptible as it perturbs more words and cost more queries. For instance, on RoBERTa-TF, the average number of queries to the model per sample increase from 625  $\rightarrow$  786.

**Advanced Adaptive / Oracle Adversary** If the adversary has full access to the model parameters, the adversary can easily generate attacks that can evade the detection method by iteratively attacking the likelihood score of RDE. Meanwhile, the adaptive adversary can apply its strategy to the extreme

<sup>5</sup>For more details regarding the experiment, see the appendix.

such that the attacked sample is completely misclassified to the incorrect target. However, we show that such contrived attacks evade RDE at a cost of high perceptibility, rendering them detectable by human inspectors or other detection methods not reliant on the features.

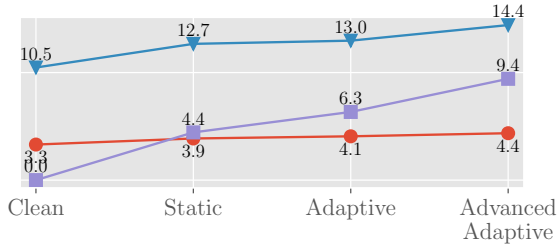


Figure 5: Comparing grammatical error (Triangle), PPL (Circle), and dissimilarity with the original sentence (Square) using USE(Cer et al., 2018)

#### 4.6 Discussion

**More Realistic Scenarios** In previous experiments, all failed adversarial attacks were discarded. However, in reality an adversary will probably have no access to the victim model so some attacks will indeed fail to fool the model and have unbalanced clean to adversarial samples. In Appendix A.11, we discuss these scenarios and provide preliminary results.

**Hyper-parameter Analysis** Although the two main hyper-parameters, support fraction ( $h$ ) of MCD and the dimension ( $P$ ), were fixed in our experiments, they can be fine-tuned in a separate validation set for optimal performance. We show in Figure 6 the performance of our method on various ranges of  $h$  and  $P$  on the validation set of IMDB-TF-BERT combination. We set  $P = 100$  and  $h$  to the default value of the algorithm when tuning for the other parameter.

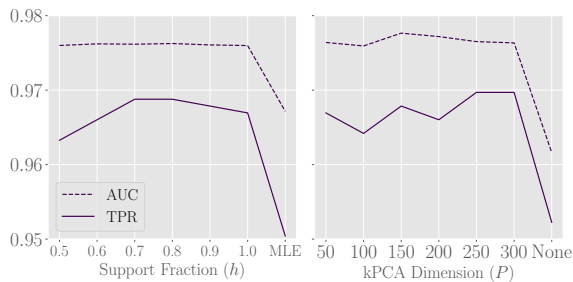


Figure 6: Hyperparameter analysis on IMDB-TF-BERT. Wide range of values all outperform the ablated forms and are relatively stable.

**Qualitative Analysis on Support Fraction** The support fraction controls the ratio of original samples to be retained by the MCD estimator, thereby controlling the volume of the contour as shown in Figure 7. We empirically demonstrated in our experiment that using all samples for parameter estimation may be detrimental for adversarial sample detection.

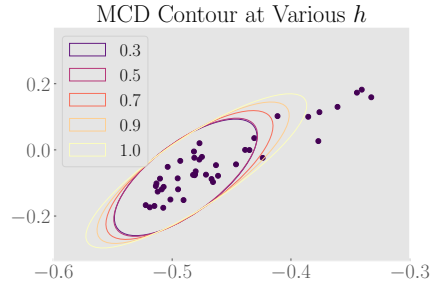


Figure 7: Qualitative example of varying support fraction  $h$  on SST2-BERT. Each ellipse represent probability contours of three standard deviations. Higher  $h$  retains more of the deviating samples and leads to wider contour.

#### 5 Related Works

In the NLP domain, few efforts have been made in detecting word-level adversarial examples. Zhou et al. (2019, DISP) utilize a detector trained on adversarial samples for a joint detect-defense system. FGWS (Mozes et al., 2021) outperforms DISP in detection by building on the observation that attacked samples are composed of rare words on 2 attack methods. Le et al. (2021) tackle a particular attack method called UniTrigger (Wallace et al., 2019), which pre-pends or appends an identical phrase in all sentences. While the performance is impressive, applying this method to other attacks requires significant adjustment due to the distinct characteristics of UniTrigger. Meanwhile, Pruthi et al. (2019) tackle character-level adversarial examples and compare with spell correctors. Our work is the first to extensively demonstrate experimental results for 4 popular and recent attack methods on 4 datasets and propose a competitive baseline. We summarize the methods in Tab. 1.

#### 6 Conclusion

We propose a general method and benchmark for adversarial example detection in NLP. Our method RDE does not require training or validation sets for each attack algorithms, yet achieves competitive performance. In the future, a principled countermeasure for an adversary with partial or full knowledge can be considered for robustness.



## References

- Theodore Wilbur Anderson. 1962. An introduction to multivariate statistical analysis. Technical report, Wiley New York.
- Rongzhou Bao, Jiayi Wang, and Hai Zhao. 2021. Defending pre-trained language models from adversarial word substitutions without performance sacrifice. *arXiv preprint arXiv:2105.14553*.
- C.M. Bishop. 1994. Novelty detection and neural network validation. *IEEE Proceedings - Vision, Image and Signal Processing*, 141:217–222(5).
- Daniel Cer, Yinfei Yang, Sheng-yi Kong, Nan Hua, Nicole Limtiaco, Rhomni St John, Noah Constant, Mario Guajardo-Céspedes, Steve Yuan, Chris Tar, et al. 2018. Universal sentence encoder. *arXiv preprint arXiv:1803.11175*.
- Jacob Devlin, Ming-Wei Chang, Kenton Lee, and Kristina Toutanova. 2018. Bert: Pre-training of deep bidirectional transformers for language understanding. *arXiv preprint arXiv:1810.04805*.
- Jerome Friedman, Trevor Hastie, and Robert Tibshirani. 2008. Sparse inverse covariance estimation with the graphical lasso. *Biostatistics*, 9(3):432–441.
- Siddhant Garg and Goutham Ramakrishnan. 2020. Bae: Bert-based adversarial examples for text classification. In *Proceedings of the 2020 Conference on Empirical Methods in Natural Language Processing (EMNLP)*, pages 6174–6181.
- Sepp Hochreiter and Jürgen Schmidhuber. 1997. Long short-term memory. *Neural computation*, 9(8):1735–1780.
- Mia Hubert, Michiel Debruyne, and Peter J Rousseeuw. 2018. Minimum covariance determinant and extensions. *Wiley Interdisciplinary Reviews: Computational Statistics*, 10(3):e1421.
- Di Jin, Zhijing Jin, Joey Tianyi Zhou, and Peter Szolovits. 2020. Is bert really robust? a strong baseline for natural language attack on text classification and entailment. In *Proceedings of the AAAI conference on artificial intelligence*, volume 34, pages 8018–8025.
- Erik Jones, Robin Jia, Aditi Raghunathan, and Percy Liang. 2020. Robust encodings: A framework for combating adversarial typos. In *Proceedings of the 58th Annual Meeting of the Association for Computational Linguistics*, pages 2752–2765.
- Yannik Keller, Jan Mackensen, and Steffen Eger. 2021. BERT-defense: A probabilistic model based on BERT to combat cognitively inspired orthographic adversarial attacks. In *Findings of the Association for Computational Linguistics: ACL-IJCNLP 2021*, pages 1616–1629, Online. Association for Computational Linguistics.
- Yoon Kim. 2014. Convolutional neural networks for sentence classification. *CoRR*, abs/1408.5882.
- Thai Le, Noseong Park, and Dongwon Lee. 2021. A sweet rabbit hole by darcy: Using honeypots to detect universal trigger’s adversarial attacks. In *59th Annual Meeting of the Association for Comp. Linguistics (ACL)*.
- Olivier Ledoit and Michael Wolf. 2004. A well-conditioned estimator for large-dimensional covariance matrices. *Journal of multivariate analysis*, 88(2):365–411.
- Kimin Lee, Kibok Lee, Honglak Lee, and Jinwoo Shin. 2018. A simple unified framework for detecting out-of-distribution samples and adversarial attacks. *Advances in neural information processing systems*, 31.
- Linyang Li, Ruotian Ma, Qipeng Guo, Xiangyang Xue, and Xipeng Qiu. 2020. Bert-attack: Adversarial attack against bert using bert. In *Proceedings of the 2020 Conference on Empirical Methods in Natural Language Processing (EMNLP)*, pages 6193–6202.
- Yinhan Liu, Myle Ott, Naman Goyal, Jingfei Du, Mandar Joshi, Danqi Chen, Omer Levy, Mike Lewis, Luke Zettlemoyer, and Veselin Stoyanov. 2019. Roberta: A robustly optimized bert pretraining approach. *arXiv preprint arXiv:1907.11692*.
- Andrew L. Maas, Raymond E. Daly, Peter T. Pham, Dan Huang, Andrew Y. Ng, and Christopher Potts. 2011. Learning word vectors for sentiment analysis. In *Proceedings of the 49th Annual Meeting of the Association for Computational Linguistics: Human Language Technologies*, pages 142–150, Portland, Oregon, USA. Association for Computational Linguistics.
- John Morris, Eli Lifland, Jack Lanchantin, Yangfeng Ji, and Yanjun Qi. 2020a. Reevaluating adversarial examples in natural language. In *Proceedings of the 2020 Conference on Empirical Methods in Natural Language Processing: Findings*, pages 3829–3839.
- John Morris, Eli Lifland, Jin Yong Yoo, Jake Grigsby, Di Jin, and Yanjun Qi. 2020b. Textattack: A framework for adversarial attacks, data augmentation, and adversarial training in nlp. In *Proceedings of the 2020 Conference on Empirical Methods in Natural Language Processing: System Demonstrations*, pages 119–126.
- Maximilian Mozes, Pontus Stenetorp, Bennett Kleinberg, and Lewis Griffin. 2021. Frequency-guided word substitutions for detecting textual adversarial examples. In *Proceedings of the 16th Conference of the European Chapter of the Association for Computational Linguistics: Main Volume*, pages 171–186.
- Nikola Mrkšić, Diarmuid O Séaghdha, Blaise Thomson, Milica Gašić, Lina Rojas-Barahona, Pei-Hao Su, David Vandyke, Tsung-Hsien Wen, and Steve Young. 2016. Counter-fitting word vectors to linguistic constraints. *arXiv preprint arXiv:1603.00892*.

680	F. Pedregosa, G. Varoquaux, A. Gramfort, V. Michel,	Thomas Wolf, Lysandre Debut, Victor Sanh, Julien	733
681	B. Thirion, O. Grisel, M. Blondel, P. Prettenhofer,	Chaumond, Clement Delangue, Anthony Moi, Pier-	734
682	R. Weiss, V. Dubourg, J. Vanderplas, A. Passos,	ric Cistac, Tim Rault, Rémi Louf, Morgan Funtow-	735
683	D. Cournapeau, M. Brucher, M. Perrot, and E. Duch-	icz, Joe Davison, Sam Shleifer, Patrick von Platen,	736
684	esnay. 2011. Scikit-learn: Machine learning in	Clara Ma, Yacine Jernite, Julien Plu, Canwen Xu,	737
685	Python. <i>Journal of Machine Learning Research</i> ,	Teven Le Scao, Sylvain Gugger, Mariama Drame,	738
686	12:2825–2830.	Quentin Lhoest, and Alexander M. Rush. 2020.	739
		<a href="#">Transformers: State-of-the-art natural language pro-</a>	740
687	Princeton. 2010. Princeton university "about wordnet."	cessing. In <i>Proceedings of the 2020 Conference on</i>	741
688	wordnet.	<i>Empirical Methods in Natural Language Processing:</i>	742
		<i>System Demonstrations</i> , pages 38–45, Online. Asso-	743
689	Danish Pruthi, Bhuwan Dhingra, and Zachary C Lip-	ciation for Computational Linguistics.	744
690	ton. 2019. Combating adversarial misspellings with		
691	robust word recognition. In <i>Proceedings of the</i>	Cihang Xie, Yuxin Wu, Laurens van der Maaten,	745
692	<i>57th Annual Meeting of the Association for Compu-</i>	Alan L Yuille, and Kaiming He. 2019. Feature de-	746
693	<i>tational Linguistics</i> , pages 5582–5591.	noising for improving adversarial robustness. In	747
		<i>Proceedings of the IEEE/CVF Conference on Com-</i>	748
694	Alec Radford, Jeffrey Wu, Rewon Child, David Luan,	<i>puter Vision and Pattern Recognition</i> , pages 501–	749
695	Dario Amodei, Ilya Sutskever, et al. 2019. Language	509.	750
696	models are unsupervised multitask learners. <i>OpenAI</i>		
697	<i>blog</i> , 1(8):9.	Weilin Xu, David Evans, and Yanjun Qi. 2018. Feature	751
		squeezing: Detecting adversarial examples in deep	752
698	Shuhuai Ren, Yihe Deng, Kun He, and Wanxiang Che.	neural networks. <i>Network and Distributed Systems</i>	753
699	2019. Generating natural language adversarial exam-	<i>Security Symposium</i> .	754
700	ples through probability weighted word saliency.		
701	In <i>Proceedings of the 57th annual meeting of the as-</i>	Wei Emma Zhang, Quan Z Sheng, Ahoud Alhazmi,	755
702	<i>sociation for computational linguistics</i> , pages 1085–	and Chenliang Li. 2020. Adversarial attacks on	756
703	1097.	deep-learning models in natural language process-	757
		ing: A survey. <i>ACM Transactions on Intelligent Sys-</i>	758
704	Peter J Rousseeuw. 1984. Least median of squares re-	<i>tems and Technology (TIST)</i> , 11(3):1–41.	759
705	gression. <i>Journal of the American statistical associ-</i>		
706	<i>ation</i> , 79(388):871–880.	Xiang Zhang, Junbo Zhao, and Yann LeCun. 2015.	760
		Character-level convolutional networks for text clas-	761
707	Peter J Rousseeuw and Katrien Van Driessen. 1999. A	sification. <i>Advances in neural information process-</i>	762
708	fast algorithm for the minimum covariance determi-	<i>ing systems</i> , 28:649–657.	763
709	nant estimator. <i>Technometrics</i> , 41(3):212–223.		
		Yi Zhou, Xiaoqing Zheng, Cho-Jui Hsieh, Kai-Wei	764
710	Bernhard Schölkopf, Alexander Smola, and Klaus-	Chang, and Xuan-Jing Huang. 2021. Defense	765
711	Robert Müller. 1997. Kernel principal component	against synonym substitution-based adversarial at-	766
712	analysis. In <i>International conference on artificial</i>	acks via dirichlet neighborhood ensemble. In <i>Pro-</i>	767
713	<i>neural networks</i> , pages 583–588. Springer.	<i>ceedings of the 59th Annual Meeting of the Associa-</i>	768
		<i>tion for Computational Linguistics and the 11th In-</i>	769
714	Bernhard Schölkopf, Alexander Smola, and Klaus-	<i>ternational Joint Conference on Natural Language</i>	770
715	Robert Müller. 1998. Nonlinear component analysis	<i>Processing (Volume 1: Long Papers)</i> , pages 5482–	771
716	as a kernel eigenvalue problem. <i>Neural computa-</i>	5492.	772
717	<i>tion</i> , 10(5):1299–1319.	Yichao Zhou, Jyun-Yu Jiang, Kai-Wei Chang, and Wei	773
		Wang. 2019. Learning to discriminate perturbations	774
718	Richard Socher, Alex Perelygin, Jean Wu, Jason	for blocking adversarial attacks in text classification.	775
719	Chuang, Christopher D. Manning, Andrew Ng, and	In <i>Proceedings of the 2019 Conference on Empirical</i>	776
720	Christopher Potts. 2013. <a href="#">Recursive deep models</a>	<i>Methods in Natural Language Processing and the</i>	777
721	<a href="#">for semantic compositionality over a sentiment tree-</a>	<i>9th International Joint Conference on Natural Lan-</i>	778
722	<a href="#">bank</a> . In <i>Proceedings of the 2013 Conference on</i>	<i>guage Processing (EMNLP-IJCNLP)</i> , pages 4904–	779
723	<i>Empirical Methods in Natural Language Processing</i> ,	4913.	780
724	pages 1631–1642, Seattle, Washington, USA. Asso-		
725	ciation for Computational Linguistics.		
726	Eric Wallace, Shi Feng, Nikhil Kandpal, Matt Gardner,		
727	and Sameer Singh. 2019. Universal adversarial trig-		
728	gers for attacking and analyzing nlp. In <i>Proceed-</i>		
729	<i>ings of the 2019 Conference on Empirical Methods</i>		
730	<i>in Natural Language Processing and the 9th Inter-</i>		
731	<i>national Joint Conference on Natural Language Pro-</i>		
732	<i>cessing (EMNLP-IJCNLP)</i> , pages 2153–2162.		

## A Appendix

### A.1 Success Rate of Attack Methods and Other Statistics

Here we briefly describe each attack method and provide some statistics about the attack results. For Table A.1, word transformation method indicates how candidate replacement words are created. Word importance ranking denotes how the ordering of which word to attack is chosen. For constraints, only those related to embedding was listed and the numbers in parenthesis denote the threshold. Higher threshold signifies stronger constraint. For more details, we refer the readers to Morris et al. (2020b). Table A.2 summarizes the attack results on three dataset for BERT. Results for other models can be found in the released dataset.

### A.2 Configuration of Adversarial Samples

Here we discuss two main configurations and their induced scenarios used in the literature. We denote the test set as  $\mathcal{X}_t$  and the correctly classified test set as  $\mathcal{X}_c \subset \mathcal{X}_t$ .

- Configuration 1 : Sample disjoint subsets  $\mathcal{S}_1, \mathcal{S}_2 \subset \mathcal{X}_t$ . For the correctly classified examples of  $\mathcal{S}_1$ , adversarial attacks are generated and the successful examples form  $\mathcal{D}_{adv}$ .  $\mathcal{D}_{clean}$  is formed from  $\mathcal{S}_2$ .
- Configuration 2 : Sample subset  $\mathcal{S} \subset \mathcal{X}_t$ . For the correctly classified examples of  $\mathcal{S}$ , adversarial attacks are generated and the successful examples form  $\mathcal{D}_{adv}$ .  $\mathcal{D}_{clean}$  is formed from  $\mathcal{S}$ .

Scenario 1 provides more flexibility in choosing the ratio between adversarial samples and clean samples, while in Scenario 2 this is determined by the attack success rate and task accuracy. For instance, an attack with low success rate will have a low adversarial-to-clean sample ratio. In addition, Scenario 2 consists of pairs of adversarial sample and its corresponding clean sample in addition to the incorrect clean samples. A more challenging scenario can be proposed by including failed attacked samples, which may be closer to the real world. Examples of failed and successful samples are provided in Table A.3.

A seminal work (Xu et al., 2018) on adversarial example detection in the image domain assumes the first scenario, whereas existing works in NLP (Le et al., 2021; Mozes et al., 2021) only experiment on the second scenario. Our benchmark framework provides the data and tools for experimenting on

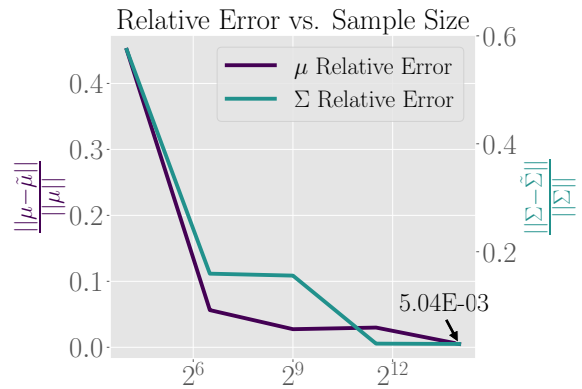


Figure A.1: Left figure shows the relative error of estimating the parameters of 768-dimensional multivariate Gaussian on a toy example. Even with  $2^{14}$  samples, the relative error of  $\mu$  is on the scale of  $10^{-3}$

both and we provide experiment results on both scenarios.

### A.3 Potential Errors of Parameter Estimation

Accurate estimation of the parameters is difficult with finite amount of samples especially in high dimensions. Here we demonstrate this through a toy example and derive its relationship with the Mahalanobis distance function, which is proportional to the likelihood. Figure A.1 shows that the MLE error remains high even when  $2^{14}$  samples are used to find the parameters of a noise-free normal distribution for both  $\mu$  and  $\Sigma$ . This, in turn, leads to an inevitably error-prone  $\tilde{\mu} = \mu - \epsilon_\mu$  and  $\tilde{\Delta} = z - \tilde{\mu}$ . Moreover, the error is amplified when computing the Mahalanobis distance due to the ill-conditioned  $\tilde{\Sigma}$  with very small eigenvalues, which is observed empirically in all datasets and models (Figure 3) possibly due to the redundant features. The (relative) condition number of the Mahalanobis distance function  $g(\Delta)$  - relative change in the output given a relative change in the inputs - is bounded by the inverse of the smallest eigenvalue of  $\tilde{\Sigma}^{-1}$ .

$$\begin{aligned} \kappa_g(\Delta) &= \frac{\|\frac{\partial g}{\partial \Delta}\|}{\|g(\Delta)\|/\|\Delta\|} \\ &= \frac{\|\Delta\|}{\|g(\Delta)\|} \|2\Sigma^{-1}\Delta\| \\ &\leq \frac{\|\Delta\|}{\|g(\Delta)\|} 2\|\Sigma^{-1}\| \|\Delta\| \end{aligned} \quad (3)$$

where the first equality follows from the definition of condition number and differentiability of  $g$  and  $C_\Delta$ . The last equality follows from the

Attacks	Citations	Word Transformation Method	Word Importance Ranking Method	Constraints
TF	204	Counter-fitted GLOVE (Mrkšić et al., 2016)	Delete Word	USE(0.84) WordEmbedding Distance(0.5)
PWWS	187	WordNet (Princeton, 2010)	Weighted Saliency	-
BAE	71	Bert Masked LM	Delete Word	USE(0.94)
TF-adj	18	Counter-fitted GLOVE	Delete Word	USE(0.98) WordEmbedding Distance(0.9)

Table A.1: Summary of attack methods and their defining characteristics.

Attacks	Post-Attack Accuracy	Attack Success Rate	Average Num. Queries
IMDB (91.9%)			
TF	0.6%	99%	558
PWWS	3%	97%	1681
BAE	34%	64%	455
TF-adj	84.2%	11%	298
AG-News (94.2%)			
TF	18%	81%	334
PWWS	41%	57%	362
BAE	82%	14%	122
TF-adj	91%	5%	56
SST-2 (92.43%)			
TF	4%	96%	91
PWWS	12%	87%	143
BAE	37%	61%	60
TF-adj	89%	5%	25

Table A.2: Summary of attack results for BERT on three datasets. Original accuracy of each dataset is written in parenthesis next to the dataset.

Caucy-Schwarz Inequality. The matrix norm induced by the L2 norm is given by the largest singular value (largest eigenvalue for a positive definite square matrix). Given the eigenspectrum of  $\Sigma$  as  $\lambda_{\max} \geq \dots \geq \lambda_{\min}$ , the eigenspectrum of  $\Sigma^{-1}$  is given by the reciprocal of that of  $\Sigma$ . Thus,  $\|\Sigma^{-1}\|$  is equal to inverse of the minimum eigenvalue of  $\Sigma$  and the last equality can be further decomposed into

$$\begin{aligned} \kappa_g(\Delta) &\leq \frac{\|\Delta\|}{\|g(\Delta)\|} 2\|\Sigma^{-1}\|\|\Delta\| \\ &\leq C_{\Delta} \frac{1}{\lambda_{\min}} \end{aligned} \quad (4)$$

where  $C_{\Delta}$  is a constant for a given  $\Delta$ . This means that when the smallest eigenvalue is in the scale of  $10^{-12}$ , even a estimation error of scale  $10^{-3}$  on  $\mu$  may be amplified by at most by a scale of  $10^9$ . This leads to a serious problem in density estimation of  $z$ .

#### A.4 More details on MCD

We explain some of the properties of the determinant of the covariance matrix. First, the determinant is directly related to the differential entropy of the

Gaussian distribution. For a  $D$ -dimensional multivariate Gaussian variable  $X$  and its probability density function  $f$ , the differential entropy is given by

$$\begin{aligned} H(X) &= - \int_{\mathcal{X}} f(x) \log f(x) dx \\ &= \frac{1}{2} \log((2\pi e)^D \det(\Sigma)) \\ &\propto \det(\Sigma) \end{aligned} \quad (5)$$

In addition, the determinant is also proportional to the volume of the ellipsoid for some  $k$ ,  $\{z \in \mathbb{R}^D : (z - \mu)^T \Sigma^{-1} (z - \mu) = k^2\}$ . We refer the readers to Section 7.5 of Anderson (1962) for the proof. This explain why the MCD estimate forms a much narrower probability contour than MLE as shown in Fig. 4.

#### A.5 Implementation Details

To meet the memory constraint of computing the kernel matrix, we sample a subset of  $\mathcal{X}_{\text{train}}$  (8,000 samples) for all experiments. All models are pre-trained models provided by TextAttack and both kPCA and MCD are implemented using scikit-learn (Pedregosa et al., 2011). We use the radial basis function as our kernel.

For subsampling generated attacks described in Section 2.2, we set the maximum number of adversarial samples for each dataset. For IMDB and AG-News, the maximum is set to 2000 and for SST-2 this is set to 1000. Then, the number of target samples (i.e.  $\|\mathcal{S}\|$  or  $\|\mathcal{S}_1\|$ ) is initialized to the maximum number divided by adversarial success ratio and task accuracy. Target sample is decremented until ratio between clean and adversarial samples can roughly be 5:5. Algorithm of RDE and MLE is provided in Algorithm 1.



SUCCESSFUL	director brian levant, who never strays far from his sitcom roots, skates blithely from one implausible[ <i>improbable</i> ] situation to another [...]	😄 → 😄
FAILED	arnold 's jump[ <i>leap</i> ] from little screen to big will leave frowns on more than a few faces	😄 → 😞

Table A.3: Successful and Failed Adv. Examples in SST2 Dataset ( original[*replaced*] )

### Algorithm 1: RDE and MLE

**Input:**  $\mathcal{X}_{\text{train}}, \mathcal{Y}_{\text{train}}, \mathcal{D} = \{\mathcal{D}_{\text{adv}}, \mathcal{D}_{\text{clean}}\}$   
**Input:** Feature Extractor  $\mathcal{H}$   
**Output:** Likelihood  $L$

- 1  $\mathcal{Z}_{\text{train}} = \mathcal{H}(\mathcal{X}_{\text{train}})$
- 2 **if** MLE **then**
- 3     **for**  $c$  **in** Class **do**
- 4          $\tilde{\mu}_c = \frac{1}{N_c} \sum_{i \in Y_c} z_i$
- 5          $\tilde{\Sigma}_c = \frac{1}{N_c} \sum_{i \in Y_c} (z_i - \tilde{\mu})(z_i - \tilde{\mu})^T$
- 6 **else if** RDE **then**
- 7      $\bar{Z} = \text{kPCA}(\mathcal{Z})$
- 8     **for**  $c$  **in** Class **do**
- 9          $\tilde{\mu}_c, \tilde{\Sigma}_c = \text{MCD}(\bar{Z}_c)$
- 10  $L = []$
- 11 **for**  $x$  **in**  $\mathcal{D}$  **do**
- 12      $z = \mathcal{H}(x)$
- 13      $\hat{y} = \text{argmax}_k \mathcal{F}(x)_k$
- 14     **if** RDE **then**
- 15          $z = \text{kPCA}(z)$
- 16      $L.append(\mathcal{N}(z | \tilde{\mu}_{\hat{y}}, \tilde{\Sigma}_{\hat{y}}))$

### A.6 Benchmark Usage Example

```

from AttackLoader import Attackloader

#Set seed, scenario, model type,
#attack type, dataset, etc.
loader = AttackLoader(...)

#Split test and validation set
loader.split_csv_to_testval()

# Subsample from testset according to
  chosen scenario
sampled, _ =
  loader.get_attack_from_csv(..)

"""
Apply detection method
"""

```

### A.7 Comparison with PCA

In all our experiments, we used a radial basis function for kPCA. This allows finding non-linear patterns in the feature space. When the linear kernel

is used, kPCA is equivalent to ordinary PCA. We demonstrate that exploiting non-linearity preserve much more meaningful information by comparing the detection performance in the IMDB dataset (Table A.5).

### A.8 ROC Curve Examples

Below (Fig. A.3) we provide Receiver Operating Characteristic (ROC) curves of RoBERTa on two attacks. For all plots, samples from the first seed are used.

### A.9 Experiment Details on Adaptive Adversary

In this section, we provide detail on the experimental settings. Instead of the terminating condition used by all attack methods

$$\mathcal{F}^*(x) = \mathcal{F}(x) \neq \mathcal{F}(x_{\text{adv}}) \quad (6)$$

the stronger attack goes on to send the sample closer to the features of the incorrect target. With fixed  $\epsilon$ , the attack terminates once

$$\mathcal{F}^*(x) = \mathcal{F}(x) \neq \mathcal{F}(x_{\text{adv}}), \quad \hat{p} > 1 - \epsilon \quad (7)$$

where  $\hat{p}$  is the largest predicted softmax probability. This allows the generated sample to fool the density-based methods that rely on the discriminative feature space. For attacks denoted 'strong'  $\epsilon = 0.1$ ; for 'stronger',  $\epsilon = 0.01$ . For RDE+, we use the adversarial samples of the held-out validation set using the static attack method.

### A.10 Detecting Character-level Attacks

Although character level attacks are perceptible to spell checkers or more sophisticated techniques (Pruthi et al., 2019), it still poses threat to deep neural networks (Zhang et al., 2020). We demonstrate the general applicability of RDE on character-level attack on 3,000 samples attacked by the character-level attack method proposed in Pruthi et al. (2019). As shown in Table A.4, RDE surpasses all the density-based methods.

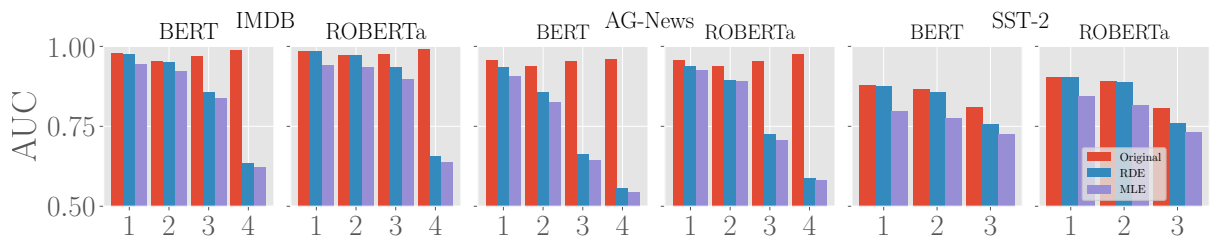


Figure A.2: Detection performance (AUC) for scenario including failed adversarial samples. Horizontal axis denotes the type of attacks methods (TF, PWWS, BAE, TF-adj). The original performance of RDE from Table 3 as an upper bound is provided (red). Blue and purple denotes RDE and MLE including failed adversarial samples, respectively.

	IMDB		AG-News	
	BERT	RoBERTa	BERT	RoBERTa
PPL	55.0±0.6	64.0±1.4	71.3±0.7	71.3±0.7
MLE	90.2±0.4	89.6±0.3	89.9±0.4	77.5±0.6
RDE	91.0±0.1	92.9±0.2	90.9±0.5	91.0±0.4

Table A.4: AUC for character level attack on AG-News averaged over five trials.

### A.11 More Realistic Scenarios

In this section, we discuss more realistic scenarios and provide preliminary results in Appendix A.11: (i) Including failed attacks (ii) Imbalanced ratio of clean and adversarial samples. In previous experiments, all failed adversarial attacks were discarded. However, in reality an adversary will probably have no access to the victim model so some attacks will indeed fail to fool the model. While failed adversarial attacks do not pose threat to the task accuracy of the model, it nevertheless may be harmful if the victim wishes to gain information about a certain population by aggregating data such as sentiment in consumer review about a movie. In addition, as active research in attacks have been made in the past few years, more subtle attacks that are imperceptible to humans naturally have lower attack success ratio (e.g. BAE).

Fig. A.2 demonstrates the detection results of RDE and MLE when distinguishing between normal samples and (failed and successful) adversarial attempts by comparing the AUC’s. As an upper bound, we provide the performance of RDE on the *original scenario* without failed adversarial examples in red. As the first two attacks (TF and PWWS) achieve nearly 100% success rate, only few failed adversarial samples are added. Accordingly, the performances for the two attacks show little difference. However, in more subtle attacks (BAE and TF-adj) the performance drastically drops due to the increased failed adversarial samples, yet RDE outperforms MLE by a considerable margin in most

cases. We end on this topic by noting that more comprehensive analysis is called for, because in some cases failed adversarial attempts are (nearly) identical to clean samples. So an attack method with low detection rate does not necessarily imply a crafty attack method in this scenario.

In Appendix Table A.7, we provide the results for Scenario 2 described in Section 2.2. The general trend among detection methods and attack methods is similar to Table 3. As noted earlier, for Scenario 2 the ratio of adversarial to clean samples will be low if the attack success rate is low. For instance, in IMDB-(TF-adj)-BERT, the ratio of adversarial to clean samples is around 1:9. Whereas both AUC and TPR are not strongly affected due to the characteristic of the metrics, F1 drastically drops. For instance, for IMDB-(TF-adj)-BERT, RDE achieves 73.7% (as opposed to 95.0% of Scenario 1). On the same set, FGWS achieves 60.1% and MLE achieves 67.6%.

Here we provide experimental results on Scenario 2. Although pairs of samples are included in the dataset, the general trend is similar to that of Scenario 1. For attack methods with low success rate, the adversarial to clean sample ratio is low, which affects the F1-score.

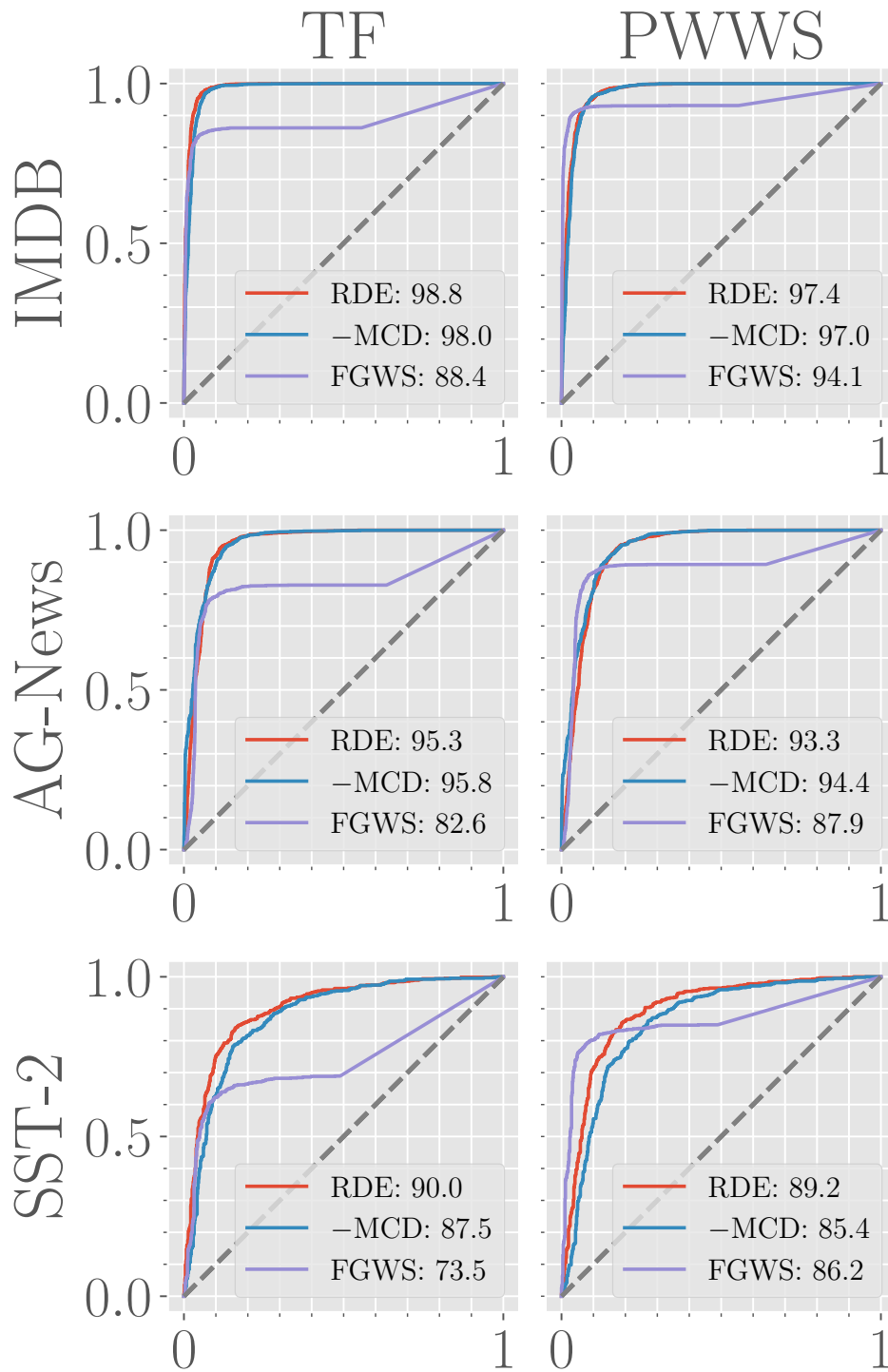


Figure A.3: ROC curves for RoBERTa on two attacks TF and PWWS. Row indicates the dataset, while the column indicates the attack methods. For all plots, the x-axis and y-axis represents FPR and TPR, respectively. The legend indicates the AUC of each methods. RDE(-MCD) is written as -MCD due to space constraint.

Models	Methods	Attacks											
		TF			PWWS			BAE			TF-adj		
		TPR	F1	AUC	TPR	F1	AUC	TPR	F1	AUC	TPR	F1	AUC
BERT	PCA	89.5±1.1	89.7±0.6	95.2±0.1	77.9±1.3	82.9±0.8	93.1±0.2	83.5±1.3	86.3±0.7	94.2±0.2	92.8±1.2	91.7±0.7	96.2±0.2
	kPCA	96.3±0.3	93.4±0.2	96.8±0.1	86.9±0.9	88.3±0.5	94.6±0.2	92.5±0.5	91.4±0.3	95.8±0.2	98.2±0.2	94.6±0.2	97.6±0.2
RoBERTa	PCA	94.7±0.6	92.5±0.3	96.3±0.1	89.7±0.9	89.9±0.5	95.4±0.1	88.2±1.3	89.0±0.7	95.0±0.3	92.6±1.8	91.6±0.9	96.7±0.5
	kPCA	98.5±0.1	94.5±0.1	97.9±0.1	95.0±0.3	92.7±0.2	96.7±0.1	95.4±0.4	93.0±0.2	97.0±0.2	98.6±0.4	94.8±0.2	98.1±0.4

Table A.5: Results of using linear kernel for KPCA, which is equivalent to the ordinary PCA on IMDB. For fair comparison, we compare with RDE(-MCD) where MCD estimation is not used. All results lead to higher performance when kPCA is used.

Models	Methods	Attacks											
		TF			PWWS			BAE			TF-adj		
		TPR	F1	AUC	TPR	F1	AUC	TPR	F1	AUC	TPR	F1	AUC
BERT	PPL	40.2±0.2	53.5±0.2	76.6±0.0	36.2±0.7	49.6±0.8	74.2±0.4	16.3±0.7	25.9±0.9	65.2±0.6	16.3±1.5	25.7±2.0	63.1±0.6
	FGWS	84.6±0.5	87.2±0.2	87.0±0.5	88.9±0.1	89.5±0.1	91.0±0.0	62.4±1.2	72.5±0.8	70.3±0.8	79.7±2.7	85.5±1.7	82.3±0.8
	MLE	41.3±1.0	54.6±1.0	66.5±0.3	41.8±0.8	55.0±0.8	66.9±0.2	42.3±1.9	55.5±1.8	67.5±0.4	38.5±2.1	52.0±2.0	66.7±0.8
	RDE	<b>97.9±0.1</b>	<b>94.3±0.1</b>	<b>96.4±0.0</b>	<b>92.7±0.5</b>	<b>91.5±0.3</b>	<b>94.9±0.1</b>	<b>97.1±0.2</b>	<b>94.0±0.1</b>	<b>96.2±0.1</b>	<b>99.8±0.1</b>	<b>95.7±0.1</b>	<b>96.4±0.1</b>
RoBERTa	PPL	38.5±0.7	51.8±0.7	73.0±0.5	36.3±0.8	49.6±0.9	71.7±0.6	17.0±0.6	26.7±0.7	60.6±0.7	12.7±1.2	20.8±1.7	58.6±0.5
	FGWS	83.5±0.1	86.5±0.1	86.6±0.1	86.8±0.2	88.3±0.1	89.7±0.1	61.9±0.6	72.6±0.4	70.9±0.4	69.1±2.7	78.7±1.7	75.6±2.3
	MLE	95.0±0.4	92.7±0.2	96.3±0.1	89.2±0.4	89.6±0.2	94.5±0.2	90.1±0.3	90.1±0.2	94.9±0.2	85.7±3.5	87.6±2.0	95.0±0.5
	RDE	<b>96.4±0.1</b>	<b>93.5±0.0</b>	<b>97.0±0.1</b>	<b>90.7±0.1</b>	<b>90.5±0.1</b>	<b>95.3±0.0</b>	<b>92.5±0.2</b>	<b>91.5±0.1</b>	<b>95.7±0.2</b>	<b>99.5±0.3</b>	<b>95.5±0.0</b>	<b>96.5±0.5</b>

Table A.6: Experiment results on the Yelp dataset

Models	Methods	Attacks											
		TF			PWWS			BAE			TF-adj		
		TPR	F1	AUC	TPR	F1	AUC	TPR	F1	AUC	TPR	F1	AUC
IMDB													
BERT	PPL	49.3±0.2	61.5±0.2	77.4±0.2	38.9±0.3	51.9±0.3	71.9±0.2	28.1±0.3	38.8±0.3	67.6±0.1	24.3±0.1	25.0±0.2	66.7±0.1
	FGWS	82.6±0.1	85.4±0.1	85.1±0.1	86.6±0.1	87.7±0.1	89.3±0.1	60.6±0.2	68.5±0.2	69.3±0.2	71.3±0.2	60.1±0.2	76.6±0.1
	MLE	86.4±1.2	87.6±0.7	94.6±0.1	76.1±1.7	81.3±1.1	92.6±0.2	82.0±0.6	82.6±0.3	93.7±0.1	87.0±0.2	67.6±0.2	95.0±0.0
	RDE(-MCD)	96.0±0.4	92.8±0.2	96.6±0.1	86.2±0.8	87.5±0.5	94.4±0.1	92.1±0.3	88.3±0.2	95.6±0.1	98.5±0.0	73.4±0.0	97.5±0.0
RDE	96.8±0.2	93.2±0.1	97.7±0.1	87.4±0.5	88.1±0.3	95.1±0.2	93.3±0.3	89.0±0.1	96.8±0.1	98.8±0.0	73.7±0.1	98.6±0.0	
RoBERTa	PPL	49.5±0.4	61.8±0.3	78.9±0.3	45.1±0.2	57.9±0.2	76.5±0.2	26.9±0.1	37.9±0.1	67.6±0.1	26.6±0.4	21.3±0.3	68.1±0.3
	FGWS	83.5±0.2	86.2±0.1	86.6±0.2	91.6±0.1	90.7±0.0	93.1±0.1	60.7±0.1	69.1±0.1	69.3±0.2	66.0±0.4	46.9±0.2	72.9±0.4
	MLE	80.7±0.8	84.4±0.5	94.0±0.0	77.3±1.0	82.3±0.6	93.2±0.1	75.9±1.0	79.5±0.6	93.0±0.1	84.1±0.7	54.7±0.2	94.3±0.0
	RDE(-MCD)	98.1±0.1	94.1±0.0	97.9±0.0	94.7±0.3	92.3±0.2	96.7±0.0	95.0±0.1	90.5±0.0	96.8±0.0	98.9±0.1	61.7±0.1	97.8±0.0
RDE	98.5±0.1	94.3±0.0	98.6±0.0	94.9±0.4	92.4±0.2	97.2±0.0	94.8±0.1	90.4±0.0	97.5±0.0	99.1±0.1	62.1±0.1	98.9±0.0	
AG-News													
BERT	PPL	76.3±0.3	80.7±0.2	91.3±0.1	72.4±0.4	75.8±0.3	90.2±0.1	30.6±0.5	29.9±0.4	72.8±0.2	35.0±0.5	19.8±0.2	74.3±0.4
	FGWS	82.4±0.6	84.4±0.4	84.2±0.7	90.9±0.2	86.8±0.1	90.0±0.1	62.9±0.3	53.0±0.3	70.5±0.1	66.0±0.6	36.3±0.6	72.4±0.4
	MLE	78.2±0.4	81.8±0.3	93.5±0.0	71.4±0.3	75.3±0.2	92.3±0.1	69.9±0.3	57.4±0.1	92.2±0.0	64.0±0.5	33.4±0.4	91.1±0.1
	RDE(-MCD)	96.3±0.3	92.1±0.1	97.2±0.0	90.5±0.3	86.6±0.1	95.7±0.1	91.4±0.3	68.8±0.1	95.5±0.0	92.2±0.5	44.4±0.1	95.6±0.0
RDE	96.0±0.3	91.9±0.1	97.0±0.0	89.8±0.4	86.2±0.2	95.4±0.0	94.0±0.2	69.9±0.1	96.2±0.0	96.6±0.1	47.4±0.3	96.6±0.0	
RoBERTa	PPL	77.3±0.3	81.5±0.2	91.8±0.1	73.0±0.3	77.2±0.2	90.0±0.1	36.2±0.5	36.3±0.5	74.9±0.3	36.2±0.3	21.5±0.2	75.8±0.2
	FGWS	79.6±0.4	83.0±0.2	82.6±0.3	86.6±0.3	85.5±0.2	88.0±0.2	52.7±0.4	48.9±0.3	64.6±0.5	60.7±0.7	34.4±0.3	70.2±0.3
	MLE	81.4±0.2	84.1±0.1	94.0±0.1	78.7±0.0	80.8±0.0	93.1±0.0	68.4±0.2	59.1±0.2	91.7±0.1	62.6±0.2	34.3±0.2	90.0±0.0
	RDE(-MCD)	89.9±0.3	89.0±0.2	96.1±0.0	85.8±0.5	85.0±0.3	95.1±0.1	81.4±0.2	66.6±0.2	94.4±0.1	80.4±0.1	42.0±0.2	93.7±0.0
RDE	92.7±0.2	90.5±0.1	95.6±0.0	86.4±0.3	85.4±0.2	94.2±0.1	92.6±0.2	72.3±0.2	95.7±0.0	93.6±0.1	47.6±0.4	95.7±0.0	
SST-2													
BERT	PPL	33.4±0.5	46.2±0.6	73.1±0.1	30.4±0.5	42.6±0.5	73.1±0.0	22.2±0.1	31.7±0.1	65.7±0.0			
	FGWS	61.4±0.6	71.2±0.5	73.5±0.4	79.4±0.2	82.9±0.1	86.2±0.1	33.0±0.3	43.8±0.3	61.2±0.2			
	MLE	33.3±0.2	46.1±0.2	80.5±0.1	23.3±0.5	34.4±0.6	78.4±0.1	34.1±0.0	45.0±0.0	76.6±0.0			
	RDE(-MCD)	60.5±0.6	70.6±0.4	86.4±0.2	45.9±0.3	58.0±0.3	83.8±0.1	44.1±0.0	54.5±0.0	79.9±0.0			
RDE	66.3±0.3	74.8±0.2	87.6±0.2	53.0±0.1	64.2±0.1	85.8±0.1	47.6±0.1	57.7±0.1	80.3±0.0				
RoBERTa	PPL	35.1±0.2	48.1±0.2	74.5±0.0	33.3±0.4	45.8±0.5	74.0±0.1	21.2±0.1	30.6±0.2	64.7±0.1			
	FGWS	61.4±0.4	71.2±0.3	73.7±0.2	80.1±0.3	83.4±0.2	86.2±0.1	36.7±0.4	47.7±0.4	60.5±0.1			
	MLE	41.8±0.3	54.7±0.2	84.2±0.1	31.6±0.4	44.0±0.4	81.5±0.2	37.0±0.0	48.0±0.0	77.7±0.0			
	RDE(-MCD)	62.5±0.6	72.1±0.5	87.5±0.3	51.9±0.6	63.3±0.5	84.7±0.1	45.6±0.3	56.1±0.2	79.2±0.1			
RDE	73.3±0.6	79.6±0.4	90.4±0.2	65.7±0.3	73.9±0.2	88.5±0.1	50.9±0.1	60.6±0.1	80.2±0.1				

Table A.7: Adversarial detection results for BERT and RoBERTa on Scenario 2 on three datasets (IMDB, AG-News, SST-2). For all three metrics, higher means better.